CHAPTER V

MISCIBILITY AND SPECIFIC INTERACTION BETWEEN 17β-ESTRADIOL AND EUDRAGIT® RS SOLID DISPERSION DETERMINED BY MTDSC AND FTIR

5.1 Introduction

A monolithic matrix is the simplest system used to control drug release. The system is composed of drug homogeneously distributed in the polymer or other carrier materials (Kim, 2000a). Solid dispersion techniques, i.e. fusion method or solvent evaporation method, are generally used to distribute drug into the polymeric matrix (Serajuddin, 1999). Miscibility of drug in the polymer is an important factor indicating the uniformity of drug in the polymeric matrix either molecular dispersion in a dissolved state or regular crystallization in a crystalline state. If drug and polymer are immiscible, lack of uniformity of drug dispersion and irregular drug crystallization in the polymeric matrix will be occurred (Greenhalgh et al., 1999). Moreover, drug release from the polymeric matrix will be varied.

In polymer sciences, the miscibility of a polymer blend composed of two amorphous polymers can be determined by thermal analysis. A single T_g point is an indication of full miscibility of a polymer blend (Kuo and Chang, 2001; Kuo et al., 2001; Maldonado-Santoyo et al., 2004). Otherwise an immiscible polymer blend exhibits more than one T_g representing T_g of amorphous pure polymers used as components (Kuo and Chang, 2001). For most polymer blends, T_g of a miscible blend lies between T_g of the pure polymers and can be predicted by Gordon-Taylor equation or its modified version equation (Maldonado-Santoyo et al., 2004). Weight fractions and T_g of pure polymer components are major factors in predicting T_g of miscible polymer blends by Gordon-Taylor equation according to earlier described equation (2.16)

$$T_g = \frac{w_1 T_{g1} + K w_2 T_{g2}}{w_1 + K w_2} \qquad 2.16$$

and K can be expressed in accordance with the Simha-Boyer rule;

$$K = \frac{\rho_1 T_{g1}}{\rho_2 T_{g2}} \qquad 2.17$$

where T_{gi}, w_i, and ρ_i are the glass transition temperature, the weight fraction and the density of the pure polymer components, respectively (Schneider, 1988). In case of a polymer blend exhibiting an interaction between the pure polymer components, Gordon-Taylor equation fails to predict the T_g. Kwei equation, a modified version of Gordon-Taylor equation, has been used to predict the T_g of this

type of polymer blend (Maldonado-Santoyo et al., 2004; Schneider, 1988). Kwei equation is written as formerly described equation (2.27);

$$T_g = \frac{w_1 T_{g1} + w_2 T_{g2}}{w_1 + K w_2} + q w_1 w_2 \qquad 2.27$$

q, in the additional term, is adjustable parameter corresponding to the strength of hydrogen bonding in a polymer blend (Kuo and Chang, 2001; Kuo et al., 2001; Maldonado-Santoyo et al., 2004).

In pharmaceutical system, several drugs in a dissolved state in polymeric matrices were reported as existing in amorphous form (Satit Puttipipatkhachorn et al., 2001; Jenquin et al., 1990; Jenquin et al., 1992). This system is nearly identical with the amorphous polymer blend. Furthermore, many solid solutions of drugs in the polymeric matrices such as salicylic acid or chlorpheniramine in ERL or ERS films have exhibited the decrease of T_g when the concentrations of those in the polymeric films increase (Jenquin et al., 1990; Jenquin et al., 1992). These phenomena have been similar to those of ibuprofen or methylparaben in ERS 30D films (Wu and McGinity, 1999; Wu and McGinity, 2003). The Mixture of 17β-estradiol (E_2) in polyvinylpyrrolidone (PVP) after passing melt extrusion process has also exhibited the increase of T_g toward T_g of PVP when the concentration of PVP increases (Hülsmann et al., 2001). Few researches in pharmaceutical field have been done to explain the miscibility of drug in polymer based on the principle of Gordon-Taylor equation.

For polymer blends composed of a crystalline polymer and an amorphous polymer, the criteria for indicating the miscibility have been used not only the variation of T_g as a function of composition but also the melting point depression. The reduction of melting temperature as a function of composition and polymer-polymer interaction parameter can be analyzed by Nishi-Wang equation (Nishi and Wang, 1975) based on the Flory-Huggins theory. Nishi-Wang equation can be written as early mentioned equation;

$$T_m - T_{mb} = \frac{-T_m B V_2 \phi_1^{\,2}}{\Delta h_2} \qquad 2.43$$

where T_m and T_{mb} are melting temperatures of the crystalline polymer and the blend, respectively; B is the interaction energy density between blend components; V_2 is the molar volume of the repeating unit of the crystalline polymer; $\emptyset_1$ is the volume fraction of the amorphous polymer in the blend; Δh_2 is the heat of fusion of the crystalline polymer per mole of the repeating unit (Rostami, 2000; Pimbert et al., 2002).

The polymeric matrix containing the concentration of drug higher than its solubility in polymer exhibits the crystallization of drug in the polymeric matrix as if the blend of a crystalline polymer with an amorphous polymer. In addition, piroxicam in PVP solid dispersion has exhibited melting point depression when the proportion of

PVP increases (Tantishaiyakul et al., 1996). This phenomenon has also been found in salicylic acid in chitosan solid dispersion (Satit Puttipipatkhachorn et al., 2001). Few researches in pharmaceutical sciences have explained the reduction of melting point of drug in the polymeric matrix based on the Flory-Huggins theory. Pharmaceutical research reports have rarely been analyzed melting point depression and drug-polymer interaction parameter by using Nishi-Wang equation based on the Flory-Huggins theory.

In case of the interaction between drug and polymer occurring, the inter-associated hydrogen bond between drug and polymer should occur and can also be investigated by fourier transform infrared (FTIR) spectroscopy (He, Zhu, and Inoue, 2004).

The objectives of this study were

(i) to characterize polymorphic forms of E_2 by thermal analysis and XRPD. Although the different polymorphic forms of E_2 have been observed by thermal analysis, X-ray diffraction pattern of each polymorphic form of E_2 has not been elucidated. This work attempted to characterize X-ray diffraction pattern of each polymorphic form of E_2.

(ii) to investigate miscibility of E_2 and ERS in solid dispersion by using the principle of Gordon-Taylor equation and the Flory-Huggins theory. If the miscibility can be forecasted by these proposed theories, thermal analysis will be one of various techniques for determining the miscibility of E_2 and ERS.

(iii) and finally to examine the specific interaction between E_2 and ERS by FTIR for supporting the prediction of the miscibility by these proposed principles.

The miscibility of E_2 in ERS indicates not only how much the possibility to achieve the uniformity of E_2 in ERS solid dispersion but also how much the potential for using ERS as a release controlling agent for E_2.

5.2 Materials and Methods

5.2.1 Materials

17β-estradiol (E_2) was purchased from Fluka Chemica, Germany. Eudragit® RS PO (Röhm Pharma GmbH, Germany) was supplied as a gift by JJ Degussa, Thailand. Absolute ethanol was of a reagent grade purchased from Merck, Germany. The chemical structures of E_2 and ERS are shown in Figure 5.1.

5.2.2 Preparation of E_2 in ERS Solid Dispersions

Solid dispersions containing E_2 in ERS at concentration range of 1-90 % w/w were prepared by solvent evaporation. E_2 and ERS at specific weight ratios were dissolved in the minimum volume of absolute ethanol to get clear solution and then poured into Teflon coated plate (15.5 cm x 15.5 cm). The absolute ethanol was evaporated at room temperature. Dried samples were kept in a desiccator over silica beads for further use.

5.2.3 Physico-Chemical Characterization of E_2, ERS, and E_2 in ERS Solid Dispersions

5.2.3.1 Differential Scanning Calorimetry (DSC)

DSC was carried out using a TA Q100 with a refrigerated cooling system (TA Instruments, New Castle, DE) and nitrogen as purge gas. The calorimeter was calibrated using indium and sapphire for temperature and heat capacity, respectively. E_2 of 3.17 mg was added to standard aluminum pan with cover (closed pan) and scanned using the following heating program: heating up to 182 °C at 10 °C/min; cooling down to 0 °C at 20 °C/min; heating up to 250 °C at 10 °C/min. This heating program enabled water loss. T_g and melting points of each form of E_2 to be determined in a run.

5.2.3.2 Thermogravimetric Analysis (TGA)

TGA was carried out using a Mettler Toledo TGA apparatus (TGA/SDTA 851e, Switzerland). E_2 was added in open pan and scanned from 0-750 °C at heating rate of 5 °C/min. Weight loss was determined gravimetrically. This technique was used to investigate the change of E_2 mass as a function of temperature in order to support the events occurring in the DSC curve.

5.2.3.3 X-ray Powder Diffraction Analysis (XRPD)

XRPD was carried out using a Siemens D5000 diffractometer (Stuttgart, Germany). E_2, E_2 heated from 0-175 °C at 5 °C/min, E_2 heated from 0-180.5 °C at 5 °C/min, and E_2 heated from 0-180.5 °C at 5 °C/min, cooled down to 0 °C at 20 °C/min, finally heated up to 140 °C at 5 °C/min were scanned from 5° to

90° 2θ (sampling interval of 0.02°) using Ni-filtered Cu Kα radiation. Operating voltage and current were 40 kV and 30 mA, respectively.

5.2.3.4 Modulated Temperature Differential Scanning Calorimetry (MTDSC)

MTDSC was carried out using a TA Q100 Modulated DSC with a refrigerated cooling system (TA Instruments, New Castle, DE) and nitrogen as purge gas. E_2, ERS, and E_2 in ERS solid dispersions at concentration range of 1-90 % w/w of each were added to standard aluminum pans with covers (closed pan) and scanned using two heating programs. Heating program I: heating from 25 to 120 °C at 10 °C/min, cooling down to 25 °C at 20 °C/min, an isothermal period for 5 min at 25 °C, and finally heating to 250 °C at 5 °C/min. Heating program II: heating from 25 to 182 °C at 10 °C/min, cooling down to 25 °C at 20 °C/min, an isothermal period for 5 min at 25 °C, and finally heating to 250°C at 5 °C/min. A modulation amplitude of ±1°C and a period of 60 s were used. MTDSC was employed to determine T_g and E_2 melting point in solid dispersions because of the advantage of MTDSC over DSC for distinguishing overlapping thermal events of E_2 and ERS.

5.2.3.5 Fourier Transform Infrared Spectroscopy (FTIR)

FTIR spectra of ERS, E_2 and solid dispersions containing 20, 50 and 75 % w/w E_2 in ERS both not heated and heated from 0-175 °C at 5 °C/min were performed with a Perkin-Elmer FTIR Spectrum One. Potassium bromide disks were prepared by grinding 2-3 mg of the respective samples with 150 mg of dried potassium bromide. Disks of 13 mm in diameter were compressed at a pressure of 6000 Psi for 3 min. The disks were then mounted in a FTIR case and scanned from 4000 to 450 cm^{-1}. Spectrometer adjustments were: resolution of 4 cm^{-1} and sample scan of 64 times. This technique was used to determine the hydrogen bonding between E_2 and ERS in solid dispersions.

5.2.4 Mathematical Analysis

5.2.4.1 Melting Point Depression Analysis

The Nishi-Wang equation was fitted to the melting point of E_2 in ERS solid dispersions determined by MTDSC in the concentration range of 20-100 % w/w. The B value was estimated by fitting the Nishi-Wang equation to experimental data by nonlinear regression analysis (GraphPad Prism® version 4.0). Δh_2 (143.2 J/g) and T_m (179.88 °C) were obtained from the MTDSC thermogram of pure E_2. V_2 (168.99 cm^3) was calculated by summation of the volumes of the structural groups of E_2 (VanKrevelen, 1990). Density of each component was obtained from the ratio of molecular weight to molar volume. Volume fraction of ERS ($Ø_1$) was calculated from the weight fractions and densities of the components. Nine experimental data points were used for this fit. The coefficient of determination (R^2) and randomness of the residuals were used to determine the goodness of fit.

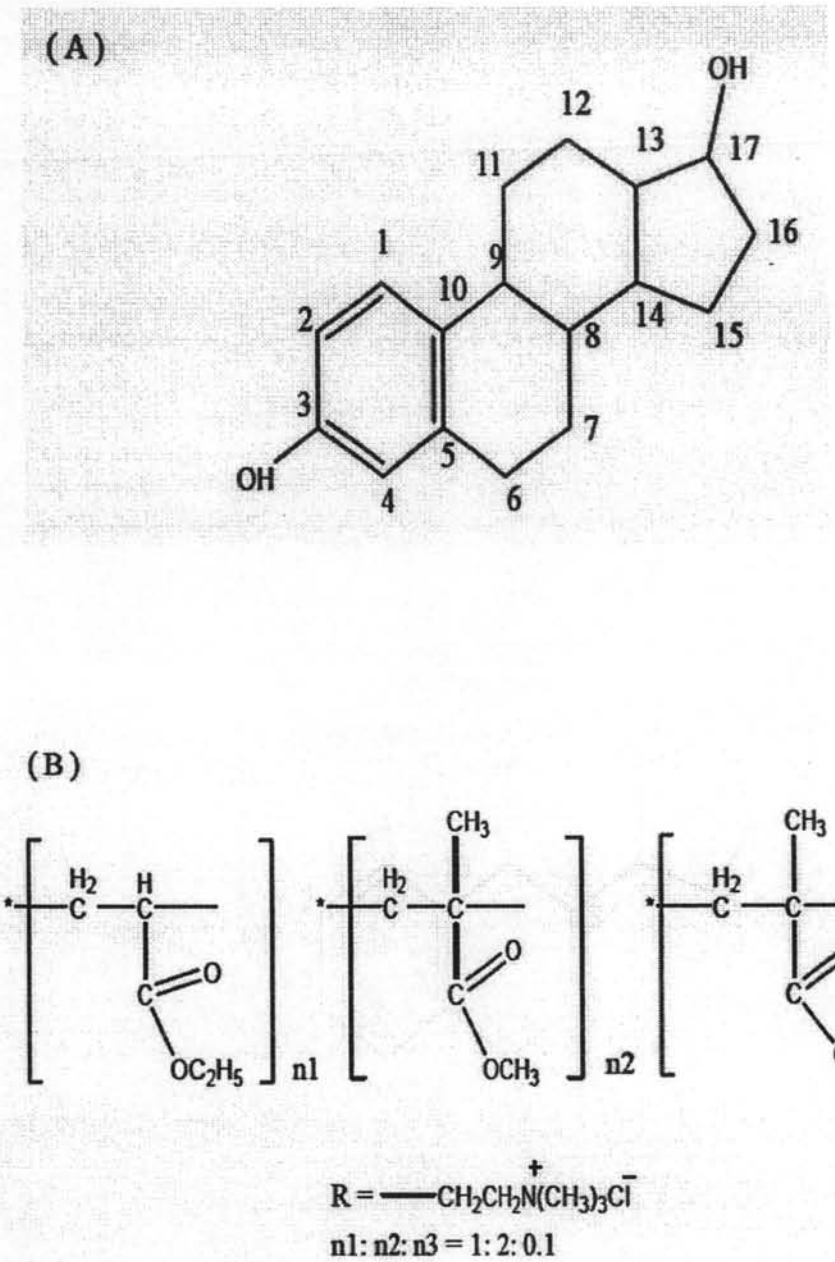

Figure 5.1 Chemical structure of E_2 (A) (Barnett et al., 1995; Variankaval et al., 2000; Park et al., 2005) **and ERS (B)** (Lehmann, 1997)

5.2.4.2 T_g Analysis

Using nonlinear regression, the Gordon-Taylor and Kwei equations were fitted to the T_g versus weight fraction of ERS (w_1) data obtained from the MTDSC thermograms of E_2 in ERS solid dispersions (0-100 % w/w). T_{g1} and T_{g2} were obtained from MTDSC thermograms of ERS and E_2, respectively. K was estimated from the Gordon Taylor fit. K and q were estimated from the Kwei fit. Thirteen experimental data points were used for each fit. The coefficient of determination (R^2) and the residual plot were used to evaluate the goodness of each fit. The best model was selected on the basis of the Akaike Infromation Criterion (AIC).

The AIC is a measurement of goodness of fit based on maximum likelihood. When comparing several models for a given set of data, the model associated with the smallest value of AIC is regarded as giving the best fit out of that set of models. The AIC value can be calculated from the below relationship;

$$AIC = n * \ln\left(\frac{SSR}{n}\right) + 2p \qquad 5.1$$

where n is the number of data points, p is the number of the estimated parameters of the model, and SSR is the residual sum of squares (Buckland, Burnham, and Augustin, 1997; Costa and Lobo, 2001).

5.3 Results and Discussion

5.3.1 DSC and TGA Curve of E_2

It has been reported that the most common form of E_2 is in hemihydrate state which is assigned to EA form according to the Variankaval et al. study (Variankaval et al., 2000). In addition, it can exist in the amorphous form and different polymorphic modifications. It is shown that crystal forms of E_2 are interconvertible by various thermal conditions. As illustrated in Figure 4.4, three endothermic peaks were observed in DSC curve of E_2 when scanned by the first heating run (DSC; 25-182 °C at 10 °C/min). The first and the second endothermic peaks were observed around 110 °C and 174 °C, respectively. These two endothermic peaks corresponded to the weight loss around 3.20 % according to the TGA curve of E_2 as illustrated in Figure 4.5. This observed water loss corresponded to the stoichiometry of E_2 given as $C_{18}H_{24}O_2.\frac{1}{2}H_2O$ which was in agreement with Variankaval et al. (2000) study. Variankaval et al. (2000) indicated that the water loss was composed of two stages. The first water loss peak after 110 °C corresponded to a partial release of hydrogen bonded water. The second peak at 174 °C corresponded to the complete loss of lattice water. The third endothermic peak at 179.24 °C was the melting point of E_2. Therefore, the DSC curve obtained from the first heating run was identical to the DSC curve of estraidol hemihydrate.

The DSC curve during cooling down (DSC; 182-0 °C at 20 °C/min) exhibited T_g of E_2 around 84.20 °C corresponding to T_g of E_2 observed in the second heating run (DSC; 0-250 °C/min at 10 °C/min). This indicated that E_2 was changed to an amorphous form after heated to 182 °C and rapidly cooled down because of manifesting T_g. In the second heating run, the amorphous form of E_2 in the glassy state was changed to the rubbery state when the temperature was higher than 80 °C. Exothermic peak in DSC curve was observed around 126 °C followed by two endothermic peaks at 169.56 °C and 179.24 °C, respectively. The first endothermic peak was lower than the second one about 10 °C. The second endothermic peak was in the same position as the third endothermic peak of the first heating run. This thermogram agreed with the result obtained by Variankaval et al. (2000) indicating that the first endothermic peak and the second endothermic peak in the second heating run were attributed by other two forms of E_2 which were assigned as ED form and EC form, respectively. It was suggested that the amorphous form of E_2 under the rubbery state crystallized to ED form and EC form at 126 °C. EC form of E_2 was in an anhydrous form because the lattice water was completely lost after the first heating run. The endothermic peak at 169.56 °C corresponding to ED form of E_2 suggested that ED form manifested itself as a mixture with EC form.

5.3.2 X-ray Powder Diffraction Pattern of E_2

X-ray powder diffraction patterns of E_2 subjected to different heat treatments are shown in Figure 5.2. E_2 without heat treatments corresponding to hemihydrate form exhibited characteristic peaks at a diffraction angle of 2θ, at 13.14, 15.74, 18.26, 22.62, and 26.58°. These diffraction angle and diffraction pattern were similar to those published by Latsch et al. (2003) and Park et al. (2005). The peaks at a diffraction angle of 2θ, at 13.60, 16.78, 21.00, and 24.72° were observed in a diffractogram of E_2 heated from 0-175 °C and 0-180.5 °C at heating rate of 5 °C/min but these peaks were not observed in a diffractogram of E_2 hemihydrate. The diffraction pattern of E_2 heated from 0-180.5 °C was nearly identical with that of E_2 heated from 0-175 °C. However, the relative peak intensity of a diffraction pattern of E_2 heated from 0-180.5 °C was less than that of E_2 heated from 0-175 °C and the peaks of a diffraction pattern of E_2 heated from 0-180.5 °C did not significantly separate from baseline. It was a sign of a mixture of crystalline form and amorphous form. This suggested that E_2 hemihydrate incompletely changed to the amorphous form after heated until the temperature reached to 180.5 °C but the lattice water was completely lost. Therefore, some portions of hemihydrate form of E_2 changed to the amorphous form and some portions of hemihydrate form of E_2 changed to the anhydrous form.

The diffraction pattern of E_2 heated from 0-180.5 °C at 5 °C/min and cooled down to 0 °C at 20 °C/min and finally heated to 140 °C at 5 °C/min was different from the others and exhibited the characteristic peaks at a diffraction angle of 2θ, at 12.64 and 19.94°. The information obtained from DSC analysis indicated that crystallization was completely occurred when the temperature reached over 140 °C and ED form was firstly obtained in the second heating run. Therefore, a diffraction pattern of E_2 obtained from this heat treatment should belong to ED form. The results

obtained from XRPD analysis confirmed the detection of three crystalline forms of E_2 as previously discussed.

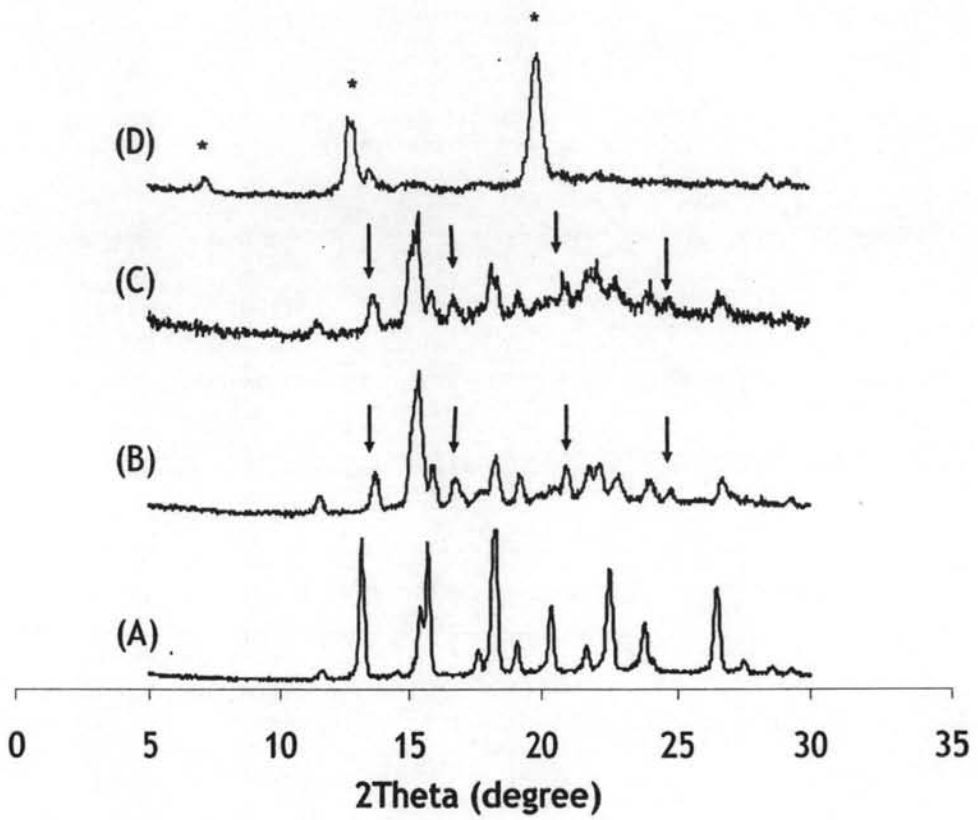

Figure 5.2 XRPD of E_2 treated with different heat treatments at heating rate of 5 °C/min: (A) no heat treatment; (B) 0-175 °C; (C) 0-180.5 °C; (D) 0-180.5 °C, 180.5-0 °C, 0-140 °C

5.3.3 MTDSC Analysis of E_2 in ERS Solid Dispersions with Heating Program I

T_g, melting point, and heat of fusion of E_2 in ERS solid dispersions at concentration range of 0-90 % w/w determined by MTDSC at heating program I are presented in Table 5.1. Pure E_2 exhibited melting point at 179.88 °C. The melting point and heat of fusion of E_2 correspondingly decreased when the concentration of ERS in solid dispersion increased. This result revealed the melting point depression as a function of composition of E_2 in ERS solid dispersion. It indicated that the miscibility of E_2 and ERS was found in the molten state. The addition of ERS as the amorphous component into the blends decreased the chemical potential of the crystalline E_2 and led to a reduction of melting point.

To investigate T_g of pure ERS and solid dispersions of E_2 in ERS, T_g was analyzed from reverse heat flow in the second heating run, MTDSC; 25-250 °C, 5 °C/min. T_g of pure ERS was found to be 68.38 °C. Each solid dispersion of E_2 in ERS at the concentration range of 1-90 % w/w exhibited only one T_g which was not significantly different from the T_g of pure ERS. In case of miscibility of E_2 and ERS, T_g of E_2 in ERS solid dispersions should lie between T_g of E_2 (84.20 °C) and T_g of ERS (68.38 °C) as a function of composition. This suggested that the resulting T_g of solid dispersions obtained from heating program I was the T_g of ERS. T_g values of E_2 in ERS solid dispersions were not altered during measurement by MTDSC using heating program I. From DSC curve of E_2 in Figure 4.4, E_2 changed to the amorphous form when heated over its melting point and rapidly cooled down. Only E_2 in the amorphous form exhibited T_g because of its amorphous nature. In heating program I, E_2 was still in the crystalline form blended with ERS. Therefore, measuring T_g of E_2 in ERS solid dispersions by MTDSC at heating program I was the measurement of T_g of ERS.

5.3.4 MTDSC Analysis of E_2 in ERS Solid Dispersions with Heating Program II

T_g values of E_2 in ERS solid dispersions at concentration range of 0-100 % w/w obtained from MTDSC using heating program II are shown in Figure 4.6 (b). T_g of pure ERS, E_2 in ERS solid dispersions, and pure E_2 were determined in the second heating run, MTDSC; 25-250 °C, 5 °C/min. Pure ERS and pure E_2 manifested their T_g at 66.21 °C and 83.77 °C, respectively. E_2 in ERS solid dispersions at concentration range of 1-90 % w/w manifested a single T_g lying between those of ERS and E_2 as a function of composition. Furthermore, T_g of E_2 in ERS solid dispersions shifted toward T_g of E_2 as weight fractions of E_2 increased. This suggested that E_2 was transformed to an amorphous state after the first heating run causing alteration of T_g of E_2 in ERS solid dispersions and the change of T_g values depended on the amount of amorphous E_2 and ERS. This drug-polymer blend was identical with the amorphous polymer blend. Therefore, T_g behavior of E_2 in ERS solid dispersion followed the principle of Gordon-Taylor equation in case of the miscibility.

Table 5.1 Glass transition temperatures (T_g), melting points (T_{mb}), and heat of fusions (Δh) of E_2 in ERS solid dispersions at concentration range of 0-100 % w/w obtained from reverse heat flow of MTDSC scanning with the heating program I

Substance	T_g (°C)	T_{mb} (°C)	Δh (J/g)
ERS	68.38	-	-
1%E_2 in ERS	68.48	-	-
2%E_2 in ERS	68.49	-	-
10%E_2 in ERS	68.99	-	-
20%E_2 in ERS	68.53	132.10	0.0860
30%E_2 in ERS	68.50	147.31	1.0930
40%E_2 in ERS	69.60	153.35	5.1840
50%E_2 in ERS	69.44	159.65	15.7300
60%E_2 in ERS	68.07	168.73	28.3000
75%E_2 in ERS	70.27	172.25	42.0500
80%E_2 in ERS	69.23	175.09	53.0500
90%E_2 in ERS	68.94	178.46	129.9000
E_2	-	179.88	143.2000

5.3.5 Melting Point Depression Analysis

Nishi-Wang equation was used to predict the melting point depression of E_2 in ERS solid dispersion. The determination of B value for E_2 in ERS solid dispersion by fitting Nishi-Wang equation to experimental data is displayed in Figure 5.3. The measured melting point of E_2 in solid dispersion (T_{mb}) was plotted against the volume fraction of ERS in solid dispersion ($\emptyset_1$). The volume fraction was obtained from converting the weight fraction into volume fraction using the molar volume of monomeric units determined by the group contribution method (VanKrevelen, 1990). The fit of Nishi-Wang equation to experimental data exhibited good agreement between predicted T_{mb} and experimental T_{mb}. The B value obtained from curve-fitting was equal to -0.2808 J/(g*cm^3). This indicated the miscibility of E_2 and ERS in solid dispersion and specific interaction between E_2 and ERS in molten state. The coefficient of determination (R^2) was 0.9804 which confirmed a good agreement between predicted T_{mb} and experimental T_{mb}. The distribution of the resulting residuals corresponding to the fit was plotted as shown in Figure 5.4. A random distribution was presented. This indicated a validity of Nishi-Wang equation to predict T_{mb} of E_2 in ERS solid dispersion.

5.3.6 T_g Analysis

Gordon-Taylor equation and its modified version equation, Kwei equation, were used to predict T_g of E_2 in ERS solid dispersion. The curve-fitting of these two equations to experimental data is presented in Figure 5.5. The measured T_g of E_2 in solid dispersion was plotted against weight percent of ERS in solid dispersion. The fit of Gordon-Taylor equation and Kwei equation to experimental data gave R^2 equal to 0.8932 and 0.9500, respectively. These values indicated that the predicted T_g values obtained from Kwei equation were better agreement with the experimental data than those obtained from Gordon-Taylor equation.

The residuals corresponding to the fit of Gordon-Taylor equation and Kwei equation to experimental data are shown in Figure 5.6 and 5.7, respectively. The residuals corresponding to the fit in Figure 5.6 and 5.7 seemed to be a kind of structure in the distribution. This was an indication of a small deviation between theory and experiment. In order to proof the validity of these models, examining runs in the time sequence plot of residuals were used (Draper and Smith, 1966). From the residuals corresponding to the fit in Figure 5.6, P-value of the cumulative distribution of the three runs in samples of sizes (4, 6) was 0.048 (Draper and Smith, 1966). This suggested that the Gordon-Taylor equation was an adequate model for explaining T_g behavior of the E_2 in ERS solid dispersions. For the residuals corresponding to the fit in Figure 5.7, P-value of the cumulative distribution of the three runs in samples of sizes (4, 7) was 0.033 (Draper and Smith, 1966). This suggested that the Kwei equation could also be used as a model for describing the T_g behavior of these solid dispersions. In order to select the best model for predicting T_g of this system, AIC values were calculated from the parameters obtained from each fit. The AIC values obtained from the fit of Gordon-Taylor and Kwei equations were 18.98 and 11.13, respectively. This indicated that Kwei equation fits the experimental data better than Gordon-Taylor equation.

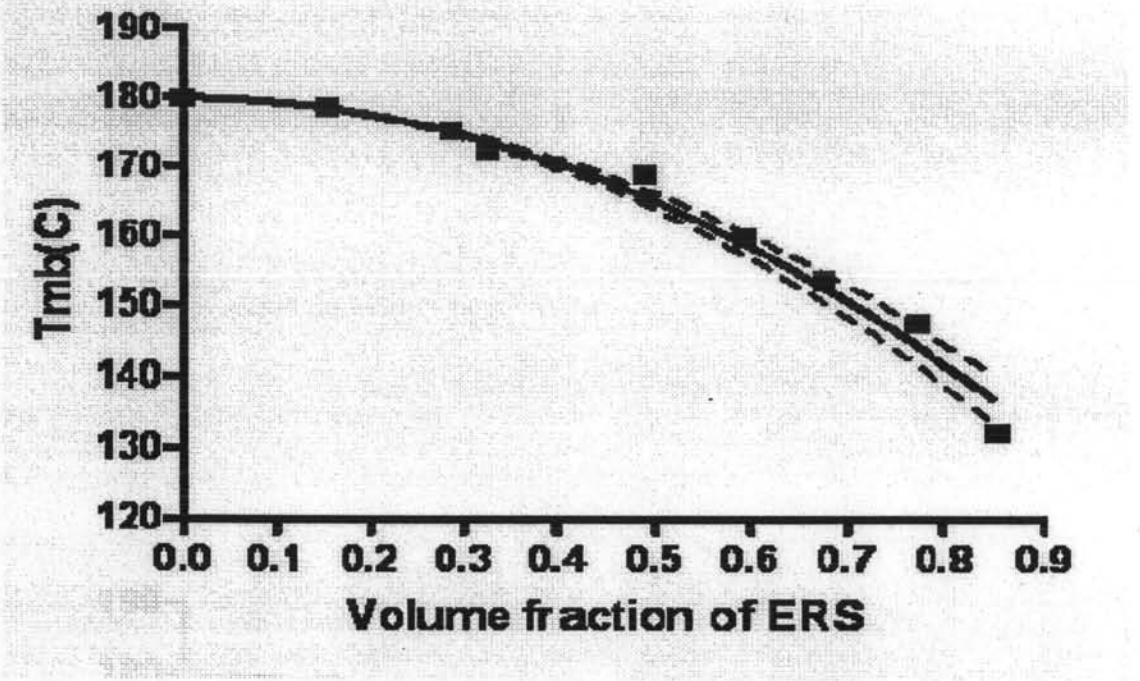

Figure 5.3 Fit of Nishi-Wang equation to experimental data: (■) T_{mb} of E_2 in ERS solid dispersions obtained from experimental data; (—) Nishi-Wang equation

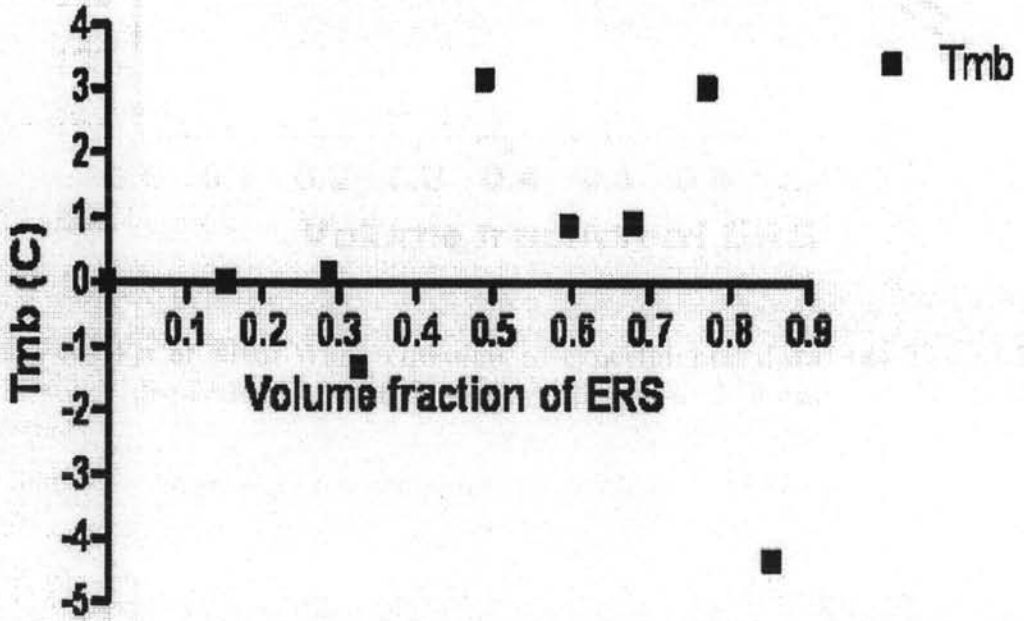

Figure 5.4 Residuals analysis corresponding to the fit of Nishi-Wang equation to experimental data

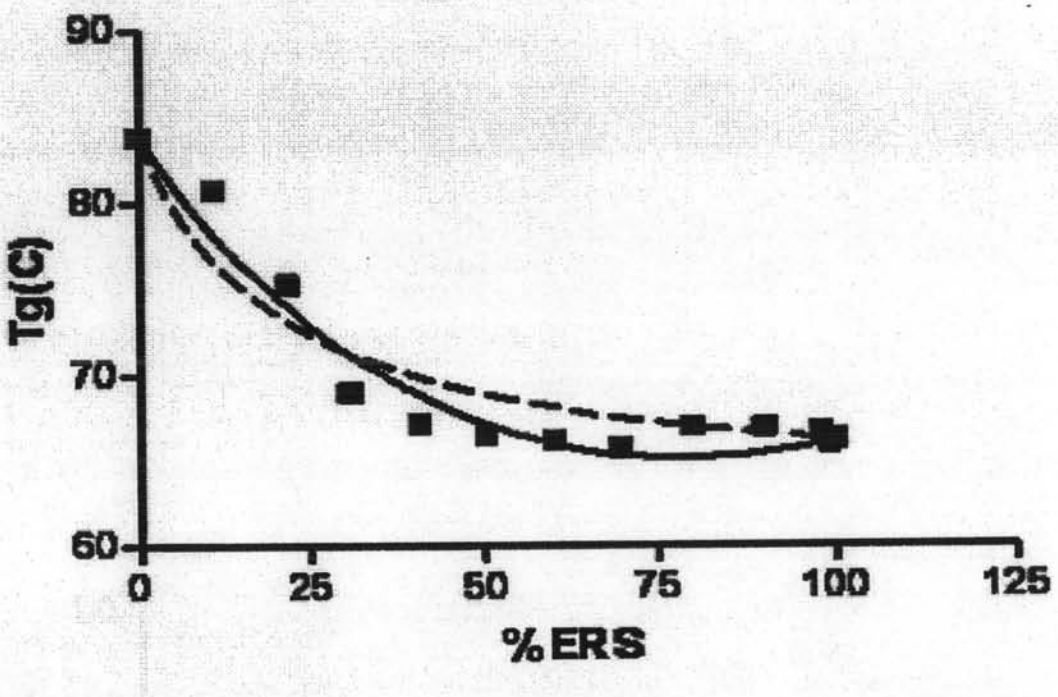

Figure 5.5 T_g versus weight fraction of ERS curves based on experimental data (■); Gordon-Taylor equation (---); Kwei equation (—)

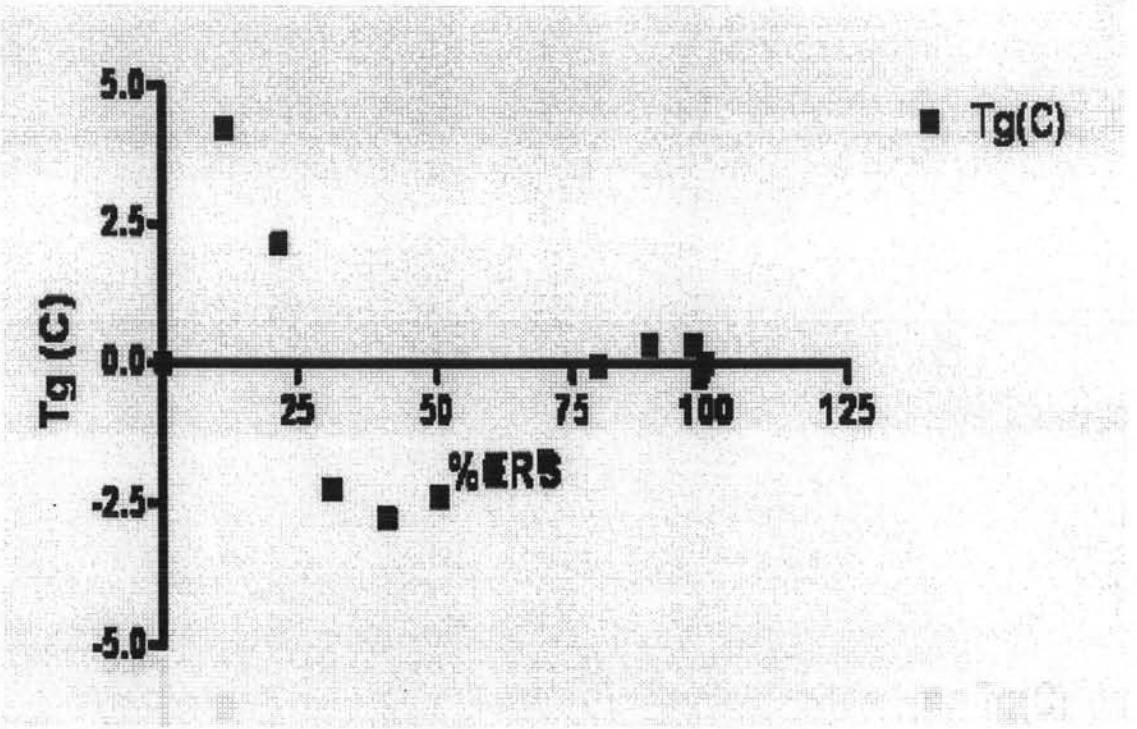

Figure 5.6 Residuals analysis corresponding to the fit of Gordon-Taylor equation to experimental data

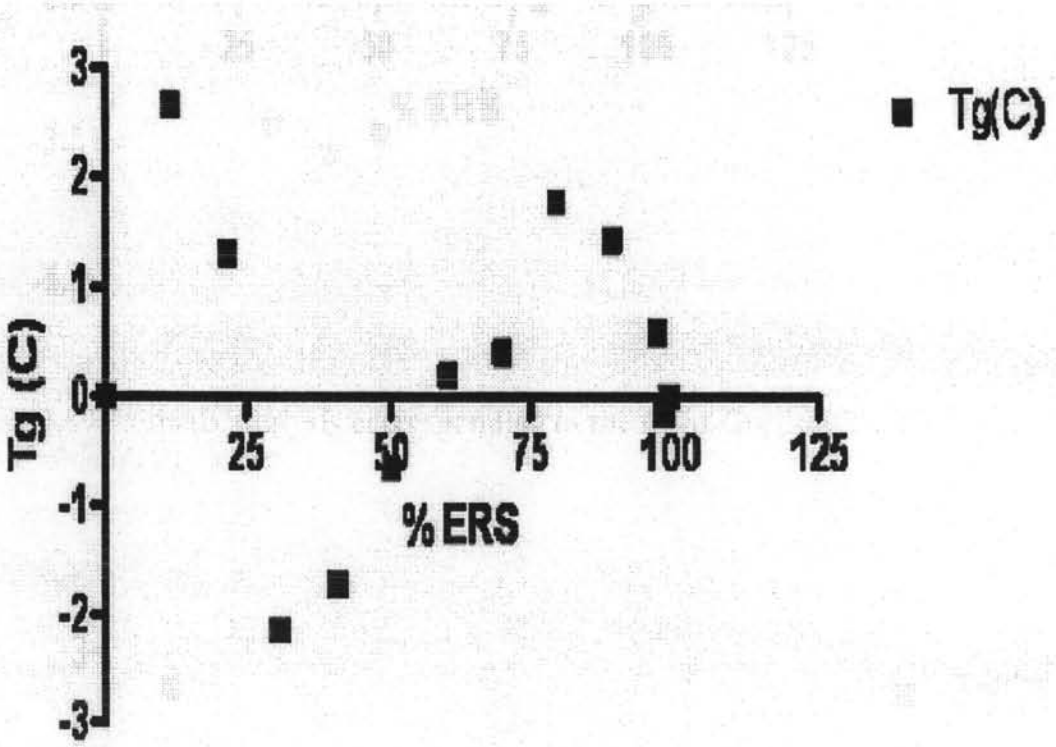

Figure 5.7 Residuals analysis corresponding to the fit of Kwei equation to experimental data

The estimate parameters, K and q values, determined from the Kwei fit were 0.4299 and –0.0017, respectively. The q value was a parameter corresponding to the strength of hydrogen bonding, reflecting the balance between breaking the self-associated hydrogen bonding and forming the inter-associated hydrogen bonding. The q value of the blend depended on an entropy change corresponding to the change in the number of hydrogen bonding. The negative q value of E_2-ERS system indicated that the fraction of the self-associated hydrogen bonding of E_2 was broken to form weaker inter-associated hydrogen bonding with ERS. The estimate parameters, q value obtained from the Kwei fit and B value obtained from the Nishi-Wang fit, were not equal to zero indicating the interaction between E_2 and ERS in the system.

5.3.7 FTIR Analysis of E_2 in ERS Solid Dispersions

FTIR spectra of E_2, E_2 in ERS solid dispersions, and ERS are displayed in Figure 5.8. Pure E_2 showed very broad bands centered at 3435.95 and 3232.06 cm^{-1} attributed to O-H stretching of hydroxyl group adjacent to C-17 and C-3 position in E_2 chemical structure, respectively. These peaks were almost the same wavenumber as those reported by Barnett et al (1995). This O-H stretching range in the FTIR spectra was sensitive to the hydrogen-bonding formation corresponding to the broad band characteristic indicating the hydrogen-bonded hydroxyl group. When adding 25 percent by weight of ERS into solid dispersion, the broad hydrogen-bonded hydroxyl bands shifted to higher frequencies at 3449.41 and 3246.95 cm^{-1} as shown in Figure 5.8 (A). However, the band at 1732 cm^{-1} corresponding to the ester C=O stretching vibration of ERS as reported by Pignatello et al. (2002) did not change when adding E_2 in solid dispersion. This suggested that hydroxyl group adjacent to C-17 and C-3 position of E_2 could not engage in inter-associated hydrogen bonding with the ester C=O group in ERS solid dispersion analyzed at room temperature. In addition, an amine salt in the ERS structure was a quaternary ammonium salt which could have no N-H stretching vibrations (Silverstein, Bessler, and Morril, 1991). Therefore, no evidence supported the inter-associated hydrogen bonding between E_2 and ERS in solid dispersion analyzed by FTIR at room temperature. Due to water inclusion of E_2 crystal, the broad bands in O-H stretching range were resulted from hydrogen-bonded hydroxyl group of E_2 with water. The shifting of these bands to higher frequencies was a result of switching from the strong hydrogen-bonded hydroxyl group of E_2 with water to the weak hydrogen-bonded hydroxyl group.

FTIR spectra of E_2 and E_2 in ERS solid dispersions heated from 25-175 °C at 5 °C/min, and ERS are shown in Figure 5.9. The peak around 3530 cm^{-1} corresponding to free hydroxyl group absorption (Kuo and Chang, 2001; Kuo et al., 2001) was observed in FTIR spectra of E_2 and 75 % w/w E_2 in ERS solid dispersion heated from 25-175 °C. Because of water loss during heating process, the free hydroxyl group of E_2 was observed. However, broad bands centered at 3434.27 and 3245.29 cm^{-1} attributed to O-H stretching of hydroxyl group adjacent to C-17 and C-3 position in E_2 chemical structure, respectively were still observed in FTIR spectrum of E_2 heated from 25-175 °C. The broad band centered at 3434.27 cm^{-1} shifted to

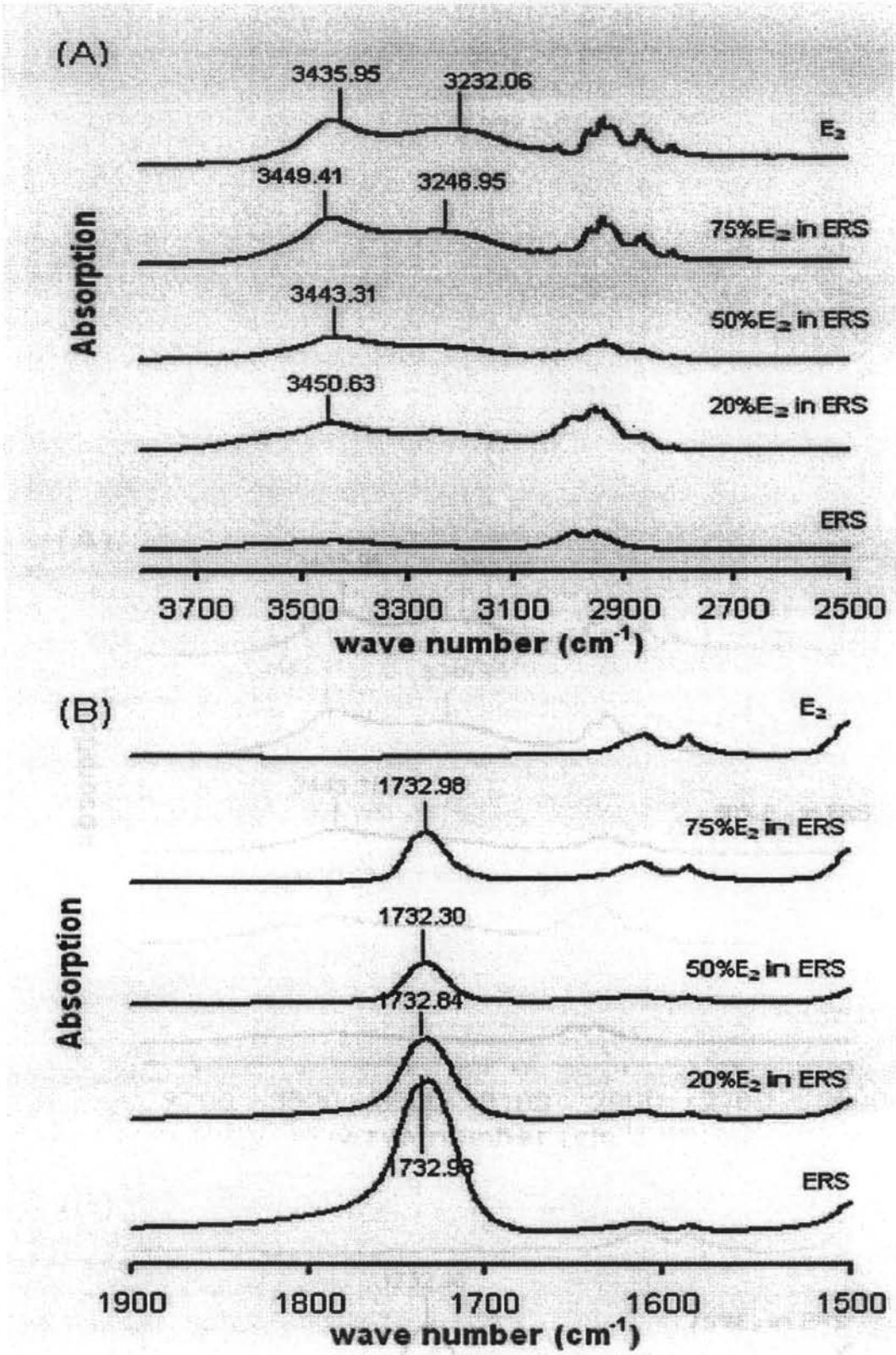

Figure 5.8 FTIR spectra of E_2 in ERS solid dispersions at concentration range of 0-100 % w/w recorded at room temperature in the range of 3800-2500 cm^{-1} (A); 1900-1500 cm^{-1} (B)

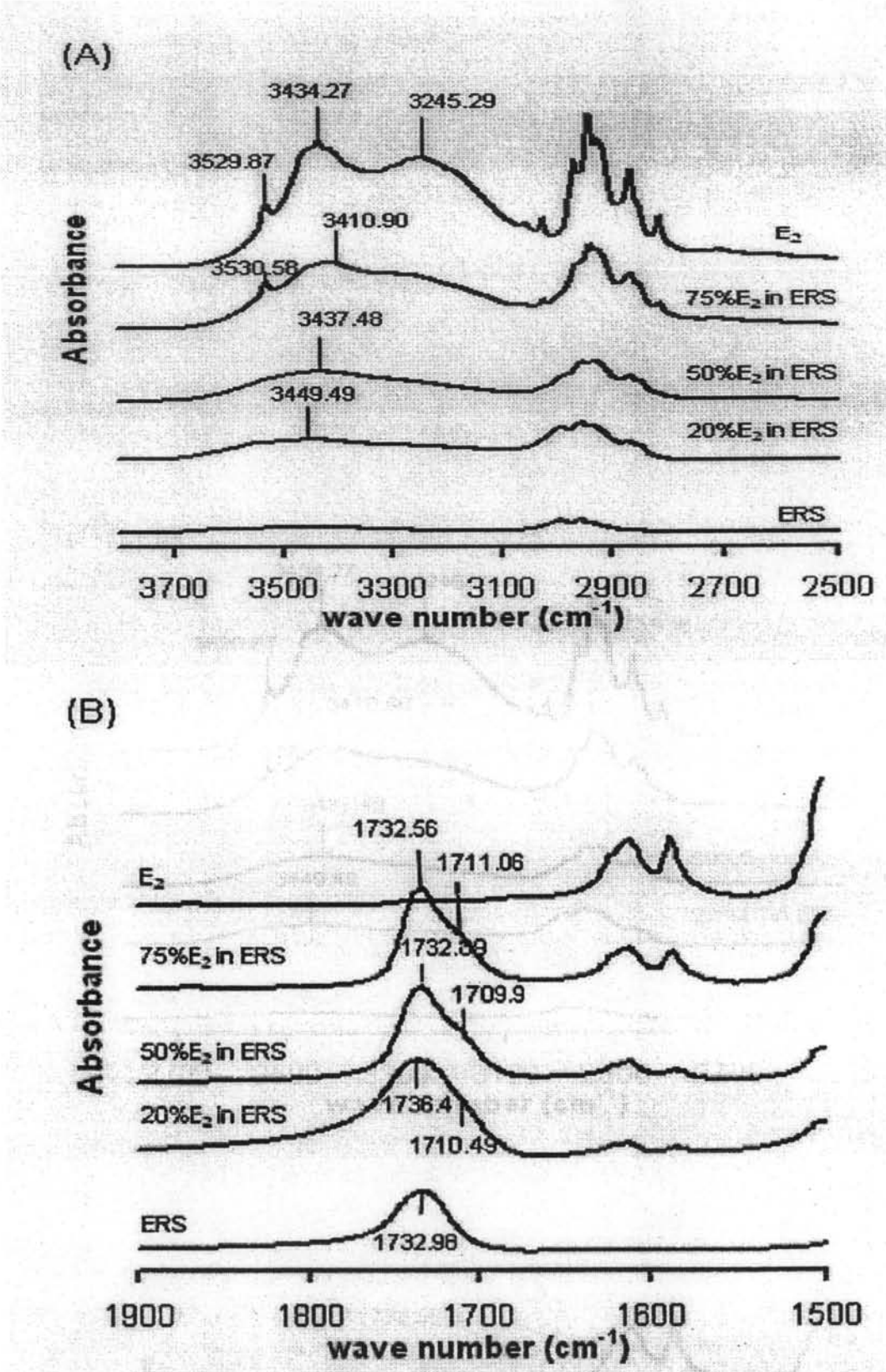

Figure 5.9 FTIR spectra of E_2 in ERS solid dispersions at concentration range of 0-100 % w/w heated from 25-175 °C at 5 °C/min and recorded at room temperature in the range of 3800-2500 cm^{-1} (A); 1900-1500 cm^{-1} (B)

3410.90 cm^{-1} corresponding to an occurrence of a shoulder of the ester C=O stretching band in FTIR spectrum of 75 % w/w E_2 in ERS solid dispersion heated from 25-175 °C. The absorption around 1732 cm^{-1} and the shoulder around 1710 cm^{-1} corresponded to the free carbonyl group and the hydrogen-bonded carbonyl group, respectively (Kuo and Chang, 2001; Kuo et al., 2001). This suggested the switching from the intra-associated hydroxyl-hydroxyl bond to the inter-associated hydroxyl-carbonyl bond.

In FTIR spectra of 50 and 20 % w/w E_2 in ERS solid dispersions heated from 25-175 °C, the peak around 3530 cm^{-1} corresponding to free hydroxyl group disappeared and the broad bands centered at 3437.48 and 3449.49 cm^{-1} were observed. This phenomenon corresponded to the shoulder around 1710 cm^{-1} of the ester C=O stretching band of ERS. This suggested the inter-associated hydrogen bonding between free hydroxyl group of E_2 and the ester C=O group of ERS when water inclusion of E_2 crystal was removed. This result was in agreement with the negative q value obtained from Kwei equation confirming the interaction between E_2 and ERS via hydrogen bonding. Moreover, this result agreed with the negative B value obtained from Nishi-Wang equation confirming the occurrence of interaction between E_2 and ERS in molten state.

5.4 Conclusions

E_2 can exist in the amorphous form and at least three crystalline forms which are interconvertible by various thermal conditions. Each polymorphic form of crystalline E_2 exhibited a XRPD pattern itself. The miscibility of E_2 and ERS in solid dispersion could be determined by MTDSC. The criteria for indicating the miscibility of polymer blends, melting point depression and a single T_g point, could be applied for indicating the miscibility of E_2 and ERS in solid dispersion. In molten state, the melting point depression as a function of composition of E_2 in ERS solid dispersion was observed. This phenomenon could be explained by Nishi-Wang equation based on the Flory-Huggins theory. For a T_g behavior, the variation of T_g as a function of composition of E_2 in ERS solid dispersion was observed when E_2 existed in an amorphous form. The variation of T_g of E_2 in ERS solid dispersion could be explained by Gordon-Taylor equation and its modified version equation, Kwei equation. Kwei equation was more appropriate than Gordon-Taylor equation to be used as a predictive model and the interaction between E_2 and ERS via inter-associated hydrogen bonding could be observed in FTIR spectra.